Automatic Pilot for Strip Processing Lines

Digital technologies are transforming industry at all levels. Steel has the opportunity to lead all heavy industries as an early adopter of specific digital technologies to improve our sustainability and competitiveness. This column is part of AIST's strategy to become the epicenter for steel's digital transformation, by providing a variety of platforms to showcase and disseminate Industry 4.0 knowledge specific for steel manufacturing, from big-picture concepts to specific processes.

Authors

Etienne Menigault
Software Development Manager, Fives KEODS, Maisons-Alfort, France

Philippe Rocabois
Metallurgist Expert, Fives KEODS, Maisons-Alfort, France

Maxime Monnoyer
Metallurgist Expert, Fives KEODS, Maisons-Alfort, France
maxime.monnoyer@fivesgroup.com

Arnaud Ollagnier
Metallurgist Expert, Fives KEODS, Maisons-Alfort, France

Aldo Fiorini
Ravenna Plant Manager, Chief Operations Officer, Carbon Steel Flat Division, Marcegaglia Ravenna SpA, Ravenna, RA, Italy

Stefano Pantarotto
Deputy Plant Manager, Marcegaglia Ravenna SpA, Ravenna, RA, Italy

Alessandro Ferraiuolo
R&D Manager, Marcegaglia Ravenna SpA, Ravenna, RA, Italy
alessandro.ferraiuolo@marcegaglia.com

Steel grade targets are defined by norms or customer specifications: mechanical properties, chemical analysis, tolerance of dimensions, surface aspect and coating properties; final treatments such as roughness, flatness, oiling or passivation are also specified with the order. The usual way to reach these targets during production on a specific continuous annealing line or a galvanizing line is to define the metallurgical road map per steel grade. These maps are usually identified as quality assurance documents and contain the chemical composition and all the process parameters from slab production to annealing time and temperature as well as skinpass elongation. These parameters are defined as validity ranges and/or as targets. Cost is considered a main parameter and must include:

- The alloy addition or liquid steel elaboration process to reach high-purity final composition such as low sulfur, low phosphorus or low carbon through a vacuum treatment.
- The productivity of the lines (mainly tons/hour).
- The technical yield such as the zinc consumption or need for head or tail cropping.
- The quality yield (percentage of final product meeting the technical requirements).
- Possibly the logistic or the purchasing cost if slabs or hot-rolled coils are supplied by distant facilities.

With such an approach, the objectives of process lines are:

- To validate the proposed ranges for each process parameter as feasible with near 100% success.
- To pilot the lines in order to respect these rules and deliver the right product all along the length and for each coil.

Rules are often adapted not only to the lines (length of each section, maximum speed, heating capacity) but also to the product thickness (cold rolling reduction ratio, minimum and maximum thickness at pickling or cold rolling mill, heating and cooling capacity, etc.). As far as possible, production planning looks for avoiding sharp and long transition linked to the inertia of the process facilities and line length: the speed is obviously uniform between loopers.

Metallurgical models have been developed over the years to simulate the product properties by varying the process parameters to optimize the process route or to check the feasibility of a specific format. These models concern a large variety of steel grades from dual-phase (DP)[1] to interstitial-free (IF)[2] and microalloyed,[3] or more recent steel grades such as quenched and partitioned (Q&P)[4] or twinning-induced plasticity (TWIP).[5] However, for an on-line operational use of the models, a limited quantity of data is necessary to operate models for the following families: low-carbon aluminum-killed, microalloyed (high-strength, low-alloy or HSLA), structural grades, IF ultralow-carbon and DP. For others, further developments must be done for an on-line operational implementation (for example, a detailed cooling and reheating pattern).

Regarding other properties, i.e., zinc thickness, roughness, flatness and surface aspects, they are

managed thanks to air knives, skinpass and zinc bath equipment. The process range for each is defined in the metallurgical road maps and the process targets tables are based on technical knowledge and permanent feedback of the production quality. Besides these tables containing ranges for each process parameters, there are some general rules, such as the maximum speed for producing a steel grade that can be lower than the maximum line speed. These rules were developed based on experience. They were usually made simple to avoid confusion for on-line personnel and non-quality issues. Therefore, they do not consider the full complexity of the incoming coil properties or the line conditions. As an example, tables are often fitted with dimension ranges regardless of the continuity and thus with potential productivity losses in the "angles" of the steps.

At least for continuous annealing or galvanizing lines, the automation of individual equipment has already been implemented, but the interaction between key process steps is often missing due to its complexity, and there are scarce links between upstream process and line control. Moreover, predefined setpoints for each process step — annealing, metallic coating, wiping and skinpass — do not allow for the complexity of the product mix to be addressed.

The approach of the SmartLine, developed by Fives, is to inverse the above logics by calculating the optimized process parameters according to each incoming full hard coil and to each product target property for each order. The SmartLine also considers and checks the consistency between each equipment in order to define the optimum in each case. Also in the case of non-uniform incoming coils, the SmartLine is able to calculate potential compensation (furnace temperature, line speed, skinpass elongation) to make it more uniform along the delivered final product.

The following section describes briefly each model and provides some of the results obtained.

Concept

The objective of the SmartLine software is to pilot the production of a galvanizing or continuous annealing line of high-quality products through the integration of the various processes including pickling, cold rolling, annealing, metallic coating and finishing target with skinpass for each coil. The continuous annealing cycle (time, temperatures) is then tailored per line (length, power, etc.) and per coil and not defined in tables per quality and dimension. This is possible through the full digital integration of the industrial processes from order to qualification and delivery in an Industry 4.0 global approach. This approach leads to a homogenization of the product properties, an optimization of the production process with an increase of the productivity and a lower energy consumption.

Data Acquisition — In order to calculate on-line the process parameters and to send results to level 1 programmable logic controllers (PLCs), a specific communication device has been developed and implemented. This device ensures the communication in real time between level 1 PLCs and level 2 models.

The model is operating as level 2. Target (material properties) and upstream (incoming coil) input information is supplied by level 3 regarding all the product details and by level 1 or level 2 regarding all the line parameters. The smart line sends calculated instruction to level 2 and level 1 of the line in real time to control the effective process parameters (line speed, furnace temperatures and power per zone, wiping and skinpass conditions).

On-Line Measurements With Tensil-Pro — A mathematical model (Tensil-Pro) developed by Marcegaglia,[6,7] is applied to the cold rolling mill and to the skinpass process, aiming to evaluate the tensile properties of the incoming and final strip (yield strength and tensile strength), the strain hardening properties ($d\sigma/d\varepsilon$), grain size and the recrystallized fraction. More recently, the possibility was developed to evaluate, by means of an additional constitutive equation, the austenite fraction formed during the annealing process just before the fast cooling.[7] Basically, the model evaluates the tensile properties using an approximated solution of Orowan equation and additional constitutive equations characterized by parameters related to physical properties of the steel under processing. The model parameters are determined for each steel grade by means of correlation analysis with the laboratory microstructure and tensile test results.

The developed methodology can be applied to carbon steel grades and other metallic alloys by adjusting the model parameters.

The on-line evaluation of flow stress is used to evaluate the ferrite grain size d_α reversing the generalized Hall-Petch equation:

$$d_\alpha = \frac{K^2}{(\sigma - \sigma_0)^2} \qquad \text{(Eq. 1)}$$

where d_α includes the friction stress, solid solution hardening and precipitation hardening, evaluated on the basis of steel chemical composition, hot rolling process, laboratory tensile tests and metallographic grain size measurements.

The calculated ferrite grain size d_α of the incoming material along the coil length is used as a main input

parameter of the predictive models used to define further the optimized annealing cycles.

Predictive Metallurgical Modeling — Most of the data are first used before production as soon as the order is allocated to a specific full hard coil with all its technical properties.

The metallurgical predictive models take into account in great detail the whole history of the product and define and anticipate the annealing, cooling and skinpassing process conditions to achieve the targeted final mechanical properties. The zinc thickness is managed thanks to a wiping model that calculates presets and makes permanent adjustments using proportional–integral–derivative (PID) regulation loop. The other properties (surface aspect, roughness, flatness, oiling) are managed through process rules often available as instruction tables.

Models are based on incoming properties along the coil length mainly to calculate the incoming grain size. The models consider:

- Recovery during heating.
- Recrystallization during heating and soaking,[8,9] based on Arrhenius law.
- Precipitation of carbides, nitrides and sulfides, if any, during heating and soaking.
- Interaction between precipitate and recrystallization to calculate the grain growth.[10]
- Phases at soaking temperature based on thermodynamics: austenite and ferrite with ratio depending on temperature, carbon content and composition using calculated Ae1, Ac1, Ac3, etc.
- Phase formed during cooling depending on initial phase(s) and cooling speed (cementite/pearlite, martensite, etc.) and eventual interactions between them, kinetics/line speed correction being applied through Johnson Mehl Avrami Kolmogorov (JMAK)[8,10] model or Hultgren[11] model for pearlite.
- Phase composition depending on chemical analysis and phase ratio.
- Solid solution hardening.
- Hardening during skinpass and tension leveler elongation using a Mecking-Kocks (MK) description for hardening[12,13] and using Grumbach law for grades with yield point elongation.[16]

Recrystallization modeling is based on JMAK:[8,10]

$$F_{ext} = \left[N_{rex}^{1/3} \left(\int_0^t M\left(X_c, X_{mn}, ..., T\right) G_{rex}\left(t\right) dt \right) \right]^n$$

(Eq. 2)

where

n = the Avrami coefficient and
F_{ext} = the extended recrystallized volume fraction.

The recrystallized volume fraction is then:

$$X = 1 - \exp\left(-X_{ext}\right)$$

(Eq. 3)

It therefore depends on:

- The net driving force for recrystallization, G(t).
- The mobility of grain boundaries, M(t).
- The volume density of nuclei available for recrystallization in the material, N_{rex}.[14]

The first two are time dependent and depend critically on the time evolution of the simultaneous recovery and precipitation processes.

The grain growth is approximated using a Hillert model:

$$d_g^{\partial} = d_r^{\partial} * \exp\frac{-Q}{RT} * t$$

(Eq. 4)

where

δ = a constant,
d_g = the grain size after grain growth and
d_r =the grain size after recrystallization.

To calculate the equilibrium austenite fraction, classical Andrews formula for Ae1, Ac1, Ac3, Ar3 and Ar1 is used as well as a level rule for ferrite and austenite fractions. It was checked that the ratio reached at equilibrium is very similar by few % to calculation by Thermocalc or JMAT-pro software. As all steel grades are low alloyed up to medium carbon (0.15%) or to DP grades, the accuracy is sufficient to calculate the final properties.

The austenite fraction is used to calculate the final ferrite grain size supposing epitaxial growth (no slow cooling section) in case of intercritical annealing temperature (two phases during soaking), or to calculate the final martensite fraction and carbon content for DP grades with fast cooling.

Mechanical properties are calculated by using an iso-work approach considering the various phases such as ferrite, martensite or pearlite[15] and using a — eventually modified — MK description for hardening[12,13] combined to a classical forest model (Taylor model):

$$\sigma = \sigma_0 + \alpha\mu bM\sqrt{\rho} \quad \text{(Eq. 5)}$$

where

σ_0 = a fixed contribution,
M = the Taylor parameter (≈3),
α = the interaction parameter between dislocations,
b = Burgers vector and
ρ = the dislocation density.

For HSLA and low-carbon aluminum-killed grades, the yield stress after skinpass is corrected by an empirical equation from Grumbach[16] considering a parabolic type of relation between the final yield stress and the skinpass deformation to eliminate the yield point elongation. For IF and DP, the increase of yield stress is calculated using the curve $d\sigma$ (constraints) versus $d\varepsilon$ (stress) from which $Rp_{0.2}$ and hardening coefficients can be deduced after the skinpass elongation. Using such an approach and considering rupture occur when Considere criterion is reached helps to deduce uniform elongation and ultimate tensile strength (UTS).

At last a machine-learning approach was applied to consider the potential weakness of a pure physical model to better fit to the industrial results. As it can be seen in Fig. 1, the final accuracy is good for yield strength (YS) and UTS of DP grades. While the physical modeling is valid for all lines, the machine learning is valid in a specific context and needs regular maintenance.

Zinc Bath Model – Regarding the zinc bath, a model is implemented to manage both the bath level and the aluminum content with the objective of keeping these values as stable as possible within a range. The future production is considered in order to anticipate both zinc and aluminum consumption based on the surface per unit time (width and forecast line speed), with zinc thickness of the next orders corresponding to about 1 hour of production.

The zinc bath mathematical model is a predictive model, providing a recommendation for the sequence of ingot feeding to be foreseen based on measured bath conditions and future production planning. The aim is to keep the zinc level and the free Al% in the Zn bath as stable as possible.

The first objective of this model is to compute the future evolution of free Al in the Zn bath considering its weight being kept constant over a defined time period and based on several inputs:

- Production schedule inputs (coil thickness, width and weight, target Zn coating weight and line speed).
- Bath conditions at time t0 (Zn bath total weight, initial bath composition, available ingot weight and composition, average skimming ratio and composition).
- Targets (target bath composition).

The model provides the user with a recommended ingot feeding sequence as an output (ingot composition, quantity and immersion time).

An initial free Al and free Fe content (wt.%) in the Zn bath is provided by laboratory or on-line measurement. Then the following elements are calculated step by step (given step duration Δt) based on the principle

Figure 1

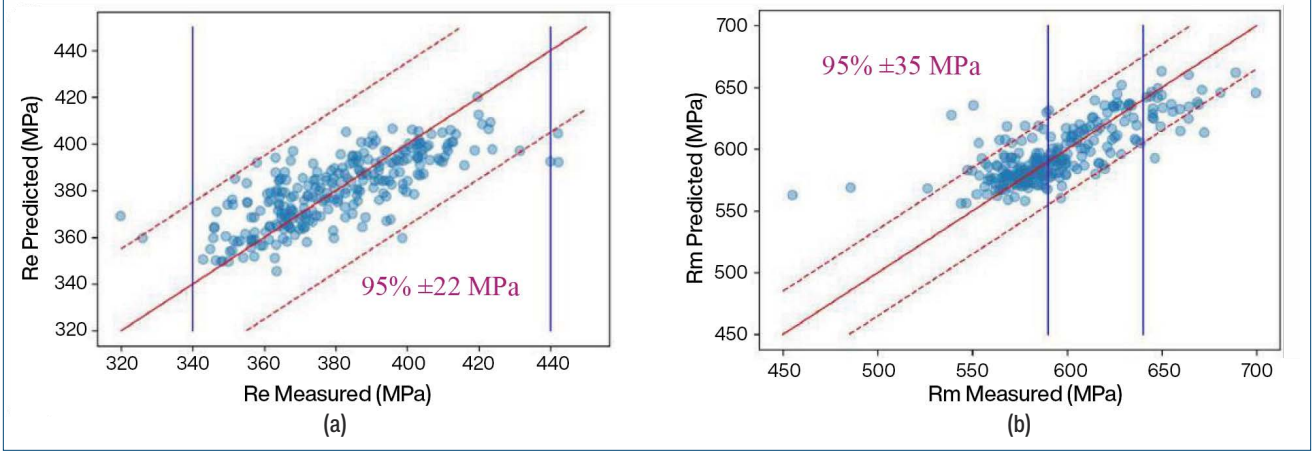

Predicted yield strength (YS) (Re) and ultimate tensile strength (UTS) (Rm) for dual-phase (DP) grades versus measured values. Except some outliers linked to process issues on coil extremity, 95% is predicted with acceptable accuracy.

Figure 2

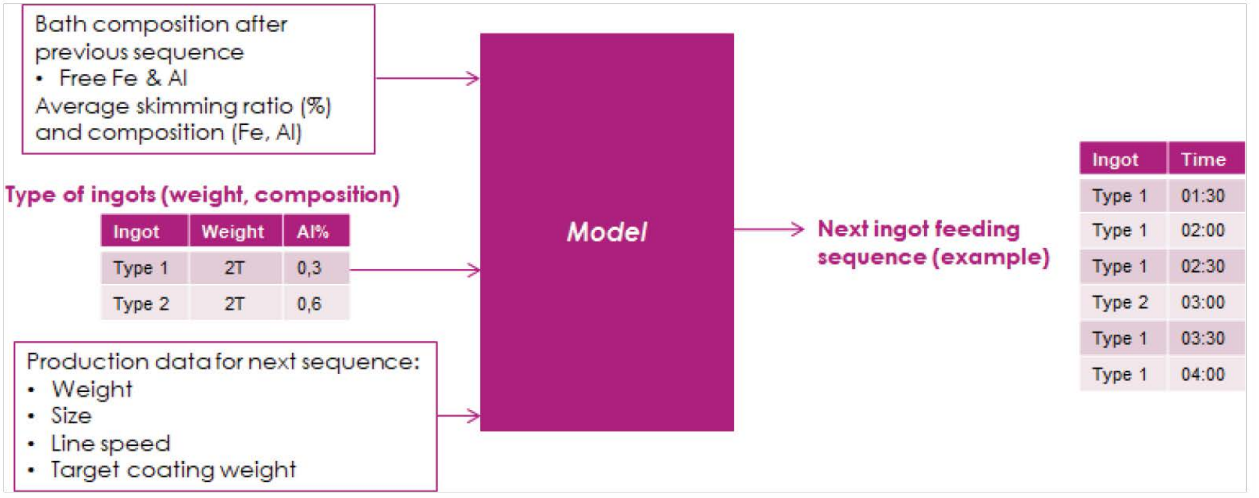

Effect Zn bath model inputs and outputs.

of global and aluminum mass balance calculation: (1) initial free Al weight in the Zn bath (measured), (2) variations of free Al and zinc weight consumption during Δt due to metallic coating consumption, skimming consumption (including dross) and Zn (Al) ingots addition; total weight of Zn bath being kept constant all the time, (3) final free Al and total weight in the bath after Δt. These final values are then reinjected as initial ones for the next calculation step.

After each calculation step Δt, the following checks are performed: (1) ingot consumption: if the current ingot is completely consumed, the model requires to add an Al-poor ingot (jumbo), (2) free aluminum content: if inferior to the Al free target, then the model requires to add an Al-rich (Zn-Al5%) ingot, eventually completing jumbo addition to keep free Al constant within given limits. The two additions are partly independent to keep the bath level and aluminum as stable as possible within defined limits.

Reset of calculation can be performed after new bath composition measurement (from laboratory on samples or on-line gauge): a new initial free Al and free Fe value is taken into consideration and the model can be run based on the next coming production schedule. Thw time of sampling is recorded and any event occurring between the sampling and the laboratory results is considered for further potential correction.

The variables used during calculation step i are $Al_{total}(t_i)$[kg] as the total variation of free Al weight in the Zn bath over $t_i - t_{i-1}$:

$$Al_{total}(t_i) = Al_{ingot}(t_i) - Al_{coating}(t_i) - Al_{intermetallic}(t_i) - Al_{skimming}(t_i)$$

(Eq. 6)

where

$Al_{ingot}(t_i)$[kg] is the variation of free Al weight in the Zn bath over Δt due to Zn ingot addition,

$Al_{coating}(t_i)$[kg] is the variation of free Al weight in the Zn bath over Δt due to metallic coating consumption,

$Al_{intermetallic}(ti)$[kg] is the variation of free Al weight in the Zn bath over Δt due to intermetallic consumption and

$Al_{skimming}(ti)$[kg] is the variation of free Al weight in the Zn bath over Δt due to skimming consumption.

At the end the calculation step i, $Al_{free}(t_{i+1})$[kg] is the weight of free Al in the Zn bath at t_{i+1}:

$$Al_{free}(t_{i+1}) = Al_{free}(t_i) + Al_{total}(t_{i+1})$$

(Eq. 7)

And using the zinc bath weight and time t_{i+1} the $\%Al_{free}$ is calculated.

The intermetallic layer of Al_2Fe_5 contains 54.7 wt.% Al and the solid zinc is supposed to contain 0.2%Al. Uncertainty coefficients will be introduced in the model to take into account: (1) inaccuracy of intermetallic layer thickness and (2) inaccuracy of Zn coating thickness.

Then the following intermediate calculations are done:

$$W_{coating}(t_i) = w(t_i) \times v(t_i) \times \Delta t \times \alpha_3 \cdot Z(t_i) \times 10^{-3}$$

(Eq. 8)

$$W_{intermetallic}(t_i) = 2 \times w(t_i) \times v(t_i) \times \Delta t \times \alpha_2 \cdot t_{Fe_2Al_5} \times 10^{-9} \times \rho_{Fe_2Al_5}$$

(Eq. 9)

$$\mathrm{Al}_{\mathrm{coating}}(t_i) = \%Al_{free}(t_i) \times W_{coating}(\Delta t)$$

(Eq. 10)

$$\mathrm{Al}_{\mathrm{intermetallic}}(t_i) = \alpha_1 \cdot \%Al_{Fe_2Al_5} \times W_{intermetallic}(\Delta t)$$

(Eq. 11)

where

$W_{coating}(t_i)$ [kg] = the total weight of coating product extracted from the bath during the time period Δt,

α_1, α_2 and α_3 = constants to be statistically fitted on a past production database.

Skimming ratio is calculated from the skimming weight and the skimming composition. The skimming composition was accurately measured over a period time used for the learning database to fit the corresponding coefficients to obtain right value of $Al_{skimming}(t_i)$:

$$W_{skimming}(t_i) = \frac{\alpha_4 \cdot \%Skimming}{1 - \alpha_5 \cdot \%Skimming} \times W_{coating}(t_i)$$

(Eq. 12)

$$Al_{skimming}(t_i) = \alpha_6 \cdot \%Al_{skimming} \times W_{skimming}(t_i)$$

(Eq. 13)

Then for computation the real content of Al of ingots is used according to their type.

Wiping Model – The first objective of the wiping model is to check that the speed proposed by the metallurgical and furnace models is feasible to reach the target zinc thickness. The second objective is to calculate a preset for distance, pressure and height of the air knives according to the target zinc thickness and line speed as proposed elsewhere.[17] The third objective is to control the pressure and distance using a PID regulation loop. The wiping model makes a diagnosis regarding the tilting or the cross-bow of the strip between the air knives.

The model relates the wiping pressure P to:

- v: strip speed.
- d: strip-nozzle distance.
- α_1 the air knives/perpendicular to strip angle (0 for horizontal).
- h: height of the air knife relative to the zinc bath.
- r: the zinc coating (target).

$$P = \frac{v^a \times \left(d \times \cos(\alpha_1)\right)^b \times h^c}{r^f}$$

(Eq. 14)

The parameters a, b, c, f and g are fitted on a database by considering only data of steady-state production. Whenever air knives are not exactly parallel to the strip, the difference of distance between strip and air knives is calculated using measured thickness on edges on both faces and the equation:

$$d_{i,j} = \left(\frac{Pr_{i,j}^f}{v^a h^c}\right)$$

(Eq. 15)

And making the average of both differences (absolute values), $|(d_{1,1} - d_{2,1})|$ and $|(d_{1,2} - d_{2,2})|$, the angle is deduced by:

$$\Delta d = \frac{|d_{1,1} - d_{2,1}| + |d_{1,2} - d_{2,2}|}{2}$$

(Eq. 16)

And the angle (for information as $d_{i,j}$ will be used for correction):

$$\alpha_2 = \arcsin\left(\frac{\Delta d}{strip\ width}\right)$$

(Eq. 17)

"d" and width must be with same dimensions in mm. To define the sign of the angle, a clear convention must be defined. Then using the opposite sign of the two differences, one can define the sign of the angle.

If convention of Fig. 3 is used: angle α_2 is negative for $(d_{1,1} < d_{2,1})$ and $(d_{1,2} > d_{2,2})$. Correction must be positive as a clockwise convention: + a2 to be applied.

Figure 3

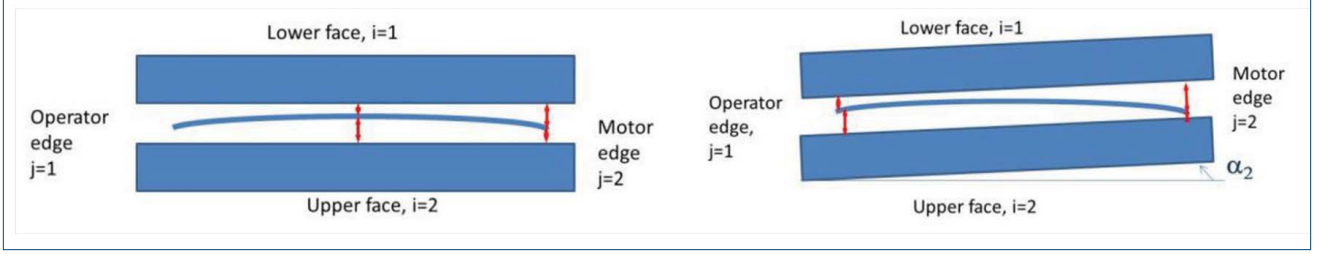

Effect of cross-bow and tilting of wiping knives or strip on various distance. The strip centering between the air knives is also a source of uneven average zinc thickness on both face.

Results

Zinc Bath – Fig. 4 reports the evolution of the free Al% content comparing the laboratory and mathematical model calculations. The laboratory analysis is carried out by means of optical emission spectrometer on lollipop samples. As it can be noted, the agreement between lab and model is quite good and the free Al% value is well controlled within the tolerances.

Table 1

Different Conditions of Zinc Thickness Measurements and Corresponding Strip Geometry Supposing the Pressure is Controlled and Uniform Across the Width. Valid if the strip is well centered by checking difference of average value per face. ≈ means similar value of zinc thickness within tolerance (for example, 5%). ">" or "<" mean different values by more than tolerance.

Conditions 1	Conditions 2	Strip/air knives
$(r_{1,1} > r_{2,1})$ and $(r_{2,2} > r_{1,2})$	$(r_{1,1} \approx r_{2,2})$ and $(r_{2,1} \approx r_{1,2})$	Not parallel angle a2 > 0
$(r_{1,1} < r_{2,1})$ and $(r_{2,2} < r_{1,2})$	$(r_{1,1} \approx r_{2,2})$ and $(r_{2,1} \approx r_{1,2})$	Not parallel angle a2 < 0
$(r_{1,1} \approx r_{1,2})$ and $(r_{2,1} \approx r_{2,2})$	$(r_{1,1} > r_{2,1})$ or $(r_{1,1} < r_{2,1})$	Cross bow, respectively, + or –
$(r_{1,1} > r_{2,1})$ and $(r_{2,2} > r_{1,2})$	$(r_{1,1} < r_{2,2})$ or $(r_{1,1} > r_{2,2})$	Cross-bow + not parallel
$(r_{1,1} < r_{2,1})$ and $(r_{2,2} < r_{1,2})$	$(r_{1,1} < r_{2,2})$ or $(r_{1,1} > r_{2,2})$	Cross-bow + not parallel

Wiping Model – Fig. 5 shows the time evolution of zinc coating amount (g/m^2) in a long sequence with different transitions in terms of coating target. As noted, the implementation of the automatic air knife control reduced significantly the under/over zinc coating typically related to strip format transitions. The actual coating control performance is below the 2% of nominal target in steady-state conditions.

Figure 4

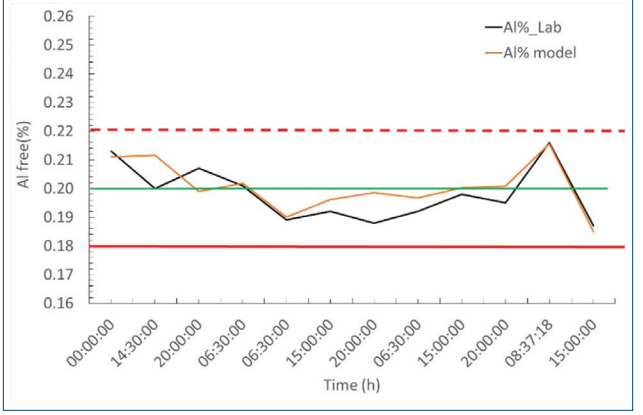

Comparison of free Al weight % as calculated by the model and as measured on samples taken in the zinc bath.

Conclusion

SmartLine uses metallurgical models for calculating process parameters. It combines models on metallurgic behavior and anticipation of the optimum processes, taking into account all parameters and requirements while also pre-empting and adjusting what is required to achieve the best possible performance. It not only automates the process, but also the complex interactions between each stage, enabling clients to achieve the best possible performance. The formula is based on the highest level of knowledge about metallurgical behavior and physical equations, combined with process analytics and designed by experts with actual steel production experience and know-how to achieve the best quality and productivity.

References

1. S.Y.P. Allain, O. Bouaziz, I. Pushkareva and C.P. Scott, "Towards the Microstructure Design of DP Steels: A Generic Size-Sensitive Mean," *Field Mechanical Model. Materials Science and Engineering A*, Vol. 637, 2015, pp. 222–234.

Figure 5

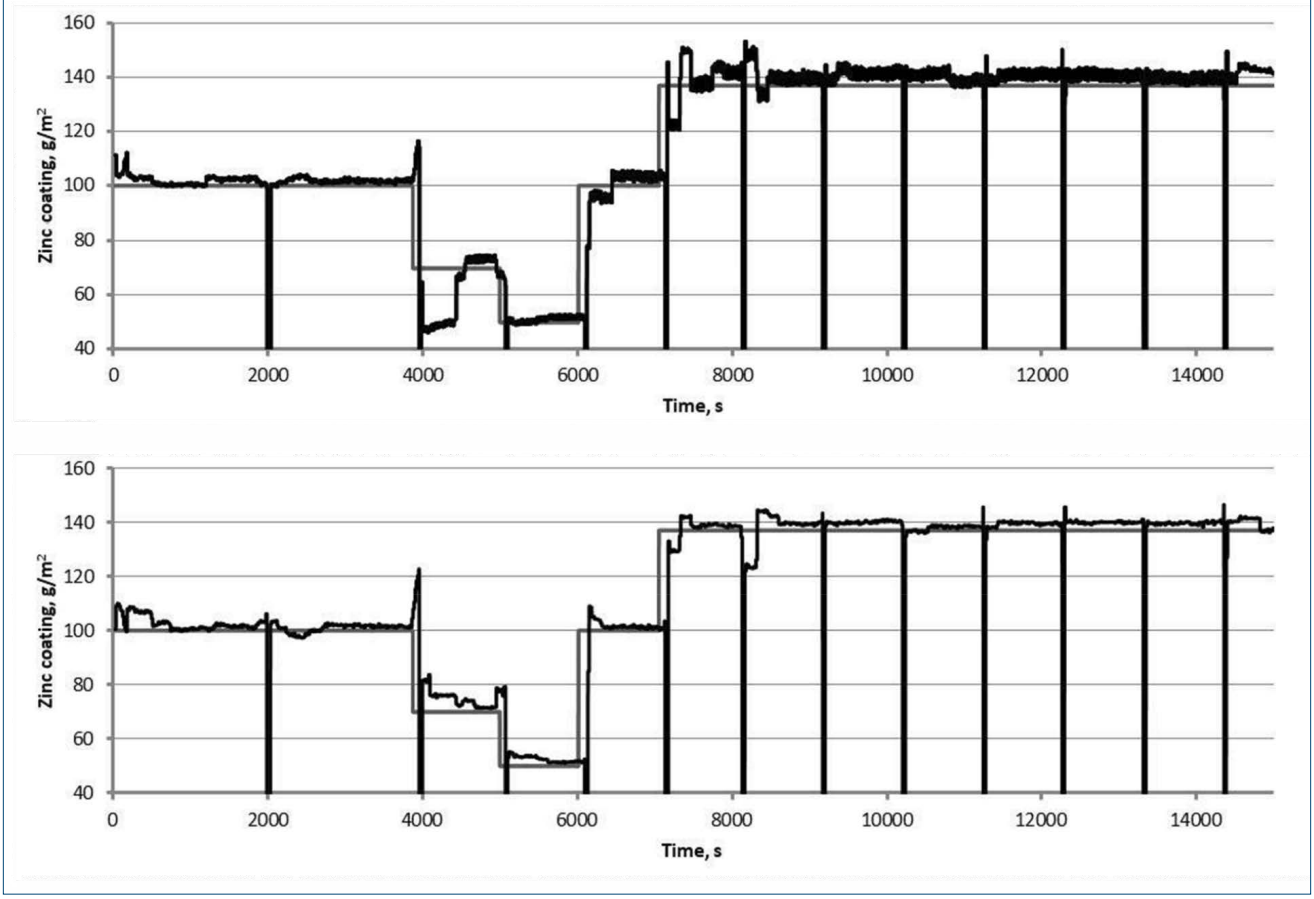

Zinc coating weight (black) as function of time with several transitions and automatic calculation of the process values (pressure, distance) according to zinc weight target (grey), line speed, wiping height. Top and bottom faces on the line. Value=0 corresponds to welds between coils where no measurement is reported.

2. H-P. Schmitz, I. Gutierezz-Sanz, E. Span, A. Schmitz, P.E. Di Nunzio, H. Palkowski, H. Réglé, G. Hribernig, "Modeling of the Impact of Chemical Composition on Important Metallurgical Processes During Cold Strip Production," Directorate-General for Research, EUR 22453 EN.
3. M. Militzer, E.B. Hawbolt and T.R. Meadowcroft, "Microstructural Model for Hot Strip Rolling of High-Strength Low-Alloy Steels," *Metallurgical and Materials Transactions A,* Vol. 31, No. 4, 2000, pp. 1247–1259.
4. A. Arlazarov, O. Bouaziz, J.P. Masse and F. Kegel, "Characterization and Modeling of Mechanical Behavior of Quenching and Partitioning Steels," *Materials Science and Engineering A,* Vol. 620, 2015, pp. 293–300.
5. O. Bouaziz, S. Allain, C.P. Scott, P. Cugy and D. Barbier, "High Manganese Austenitic Twinning Induced Plasticity Steels: A Review of the Microstructure Properties Relationships," *Current Opinion in Solid State and Materials Science,* Vol. 15, No. 4, 2011, pp. 141–168.
6. A. Ferraiuolo, "Device and Method for Online Measurement of Tensile and Microstructure Properties of Steels and Metallic Alloys," IT Patent office N. 102017000035735, 2017.
7. A. Ferraiuolo, "Online Tensile-Structure Properties Evaluation by Means of Stress-Strain Analysis of Skinpass Process Data," *METEC 4th ESTAD,* 2019.
8. A. Mathevon, V. Massardier, D. Fabrègue, P. Rocabois and M. Perez, "Extended JMAK Model for Recrystallization in Dual-Phase Steels."
9. M. Ollat, V. Massardier, D. Fabregue, F. Keovilay, E. Buscarlet and M. Perez, "Modeling of the Recrystallization and Austenite Formation Overlapping in Cold-Rolled Dual-Phase Steels During Intercritical Treatments," *Metallurgical and Materials Transactions A,* 2017, pp. 1–14.
10. H.S. Zurob, C.R. Hutchinson, Y. Brechet and G. Purdy, "Modeling Recrystallization of Microalloyed Austenite: Effect of Coupling Recovery, Precipitation and Recrystallization," *Acta Materialia,* Vol. 50, 2002, pp. 3075–3092.
11. A. Hultgren, "Isothermal Transformation of Austenite and Partitioning of Alloying Elements in Low Alloy Steels," *Tech. Rep. Series4,* Swedish Academy of Sciences, Stockholm, Sweden, 1953.
12. U.F. Kocks and H. Mecking, "Physics and Phenomenology of Strain Hardening: The FCC Case," *Progress in Materials Science*, Vol. 48, No. 3, 2003, pp. 171–273.
13. H. Mecking and U.F. Kocks, *Acta Metallurgica,* Vol. 29, 1981, p. 1865.
14. F.J. Humphreys and M. Hatherly, *Recrystallization and Related Annealing Phenomena,* Elsevier, 2004.
15. S.Y.P. Allain, O.Bouaziz, I. Pushkareva and C.P. Scott, "Towards the Microstructure Design of DP Steels: A Generic Size-Sensitive Mean-Field Mechanical Model," *Materials Science & Engineering,* Vol. A637, 2015, pp. 222–234.
16. C. Jutteau, M. Grumbach, A. Le Bon and M. Prudhomme, "Studies on Temper Rolling: Industrial Applications," *Rev. Met. Paris,* Vol. 79, No. 12, 1982, pp. 991–1006.
17. N. Guelton and A. Lerouge, "Coating Weight Control on ArcelorMittal's Galvanizing Line at Florange Works," *Control Engineering Practice,* Vol. 18, 2010, pp. 1220–1229. ✦

This paper was presented at AISTech 2021 — The Iron & Steel Technology Conference and Exposition, Nashville, Tenn., USA, and published in the AISTech 2021 Conference Proceedings.